Rate Constants and H Atom Branching Ratios of the Gas-Phase Reactions of Methylidyne CH($X^2\Pi$) Radical with a Series of Alkanes

Jean-Christophe Loison,* Astrid Bergeat, Françoise Caralp, and Yacine Hannachi

Laboratoire de Physico-Chimie Moléculaire, CNRS UMR 5803, Université Bordeaux I, F-33405 Talence Cedex, France

Received: September 7, 2006; In Final Form: October 19, 2006

The reactions of the CH radical with several alkanes were studied, at room temperature, in a low-pressure fast-flow reactor. CH($X^2\Pi$, $v = 0$) radicals were obtained from the reaction of $CHBr_3$ with potassium atoms. The overall rate constants at 300 K are $(0.76 \pm 0.20) \times 10^{-10}$ [Fleurat-Lessard, P.; Rayez, J. C.; Bergeat, A.; Loison, J. C. *Chem. Phys.* **2002**, *279*, 87],[1] $(1.60 \pm 0.60) \times 10^{-10}$[Galland, N.; Caralp, F.; Hannachi, Y.; Bergeat, A.; Loison, J.-C. *J. Phys. Chem. A* **2003**, *107*, 5419],[2] $(2.20 \pm 0.80) \times 10^{-10}$, $(2.80 \pm 0.80) \times 10^{-10}$, $(3.20 \pm 0.80) \times 10^{-10}$, $(3.30 \pm 0.60) \times 10^{-10}$, and $(3.60 \pm 0.80) \times 10^{-10}$ cm^3 $molecule^{-1}$ s^{-1}, (errors refer to $\pm 2\sigma$) for methane, ethane, propane, *n*-butane, *n*-pentane, neo-pentane, and *n*-hexane respectively. The experimental overall rate constants correspond to those obtained using a simple classical capture theory. Absolute atomic hydrogen production was determined by V.U.V. resonance fluorescence, with H production from the CH + CH_4 reaction being used as a reference. Observed H branching ratios were for CH_4, 1.00 [Fleurat-Lessard, P.; Rayez, J. C.; Bergeat, A.; Loison, J. C. *Chem. Phys.* **2002**, *279*, 87];[1] C_2H_6, 0.22 ± 0.08 [Galland, N.; Caralp, F.; Hannachi, Y.; Bergeat, A.; Loison, J.-C. *J. Phys. Chem. A* **2003**, *107*, 5419];[2] C_3H_8, 0.19 ± 0.07; C_4H_{10} (*n*-butane), 0.14 ± 0.06; C_5H_{12} (*n*-pentane), 0.52 ± 0.08; C_5H_{12} (neo-pentane), 0.51 ± 0.08; C_5H_{12} (iso-pentane), 0.12 ± 0.06; C_6H_{14} (*n*-hexane), 0.06 ± 0.04.

I. Introduction

The methylidyne radical, CH, is extremely reactive due to the presence of one singly occupied and one vacant nonbonding molecular orbitals, both localized on the C atom, allowing reactions without barriers (addition to π bonds or insertion into σ bonds). Because of its high reactivity, the CH radical plays a major role in hydrocarbon combustion,[3] in dense interstellar clouds (ISCs),[4] and in the atmospheres of Titan,[5] Neptune,[6] and Triton,[7] in which CH radicals are produced by photodissociation of CH_4.[8,9] The CH radical reactions provide a way to synthesize long chain hydrocarbons and complex organic molecules in dense interstellar clouds (ISCs)[4] and planetary atmospheres.[10] The kinetics of CH reactions with various alkanes[11−16] have been studied at temperatures ranging from 300 to 650 K and down to 23 K for CH + CH_4 and CH + C_2H_6.[17,18] There is only one experimental study for CH + neo-pentane[15] and none for other pentane isomers. For the CH + hexane reaction, there is no experimental rate constant determination to our knowledge. The experimental temperature dependences of the CH + alkane rate constants between 300 and 650 K suggest that those reactions proceed without any barrier as confirmed for the CH + CH_4 and CH + C_2H_6 reactions in the Rowe group[17,18] by kinetics studies down to 23 K. Such barrierless reactions are dominated by the long-range attractive intermolecular potential, which could also explain the variation of the rate constants with the size of the alkane. The first step in the reaction of CH with the alkane is the CH insertion either in a C−H or C−C bond, leading to an alkyl radical which then quickly evolves. Except for our studies on CH + CH_4 and CH + C_2H_6,[1,2] and one study on the reactions of CH radicals with C_2H_2, C_2H_4, C_2H_6, and CH + neo-pentane,[19] no other branching ratio determination exists. Equally, if we exclude our studies on CH + CH_4 and CH + C_2H_6 systems,[1,2] and one study on CH + CH_4 by Taatjes and Klippenstein,[20] there is no extensive theoretical study of these reactions.

We performed kinetics experiments using a selective source of CH radicals in a low-pressure fast-flow reactor at room temperature. The overall rate constants were obtained by studying the decay of the CH radical, by laser induced fluorescence (LIF), or by OH chemiluminescence after addition of a small amount of O_2 (CH + $O_2 \rightarrow$ OH($A^2\Sigma$) + CO), the alkane being introduced in excess; the diffusion corrections had been validated in previous studies.[1,2,21,22] Absolute product branching ratios of the CH + alkane reactions were estimated for the channels yielding H atoms by comparison with the CH + $CH_4 \rightarrow C_2H_4$ + H (100%) reaction,[1] the H atoms being probed by resonance fluorescence in the vacuum ultraviolet. We performed new ab initio and RRKM calculations on the CH + C_3H_8 system to assess precisely the mechanism of this reaction. To interpret the H branching ratio for the other alkane reactions, we use the results of the CH + C_3H_8 calculations, as well as our previous calculations on the CH + C_2H_6 system[2] and the extensive experimental and theoretical data on the alkyl decomposition.[23,24]

II. Experimental Measurement

The experimental setup has been described in detail previously,[1,2,21,22] and only a brief summary is given here. The setup consists of a fast-flow reactor (i.e., a 36-mm inner tube with four optical ports for detection). The CH radicals are produced in an "injector" which slides along the axis of the reactor. At the end of the injector, the CH radicals are mixed with the alkane

* To whom correspondence should be addressed. E-mail: jc.loison@lpcm.u-bordeaux1.fr. Fax: (33) 5 40 00 25 21.

10.1021/jp065831r CCC: $33.50
Published on Web 11/30/2006

flow. The distance, *d*, between the end of the injector and the observation windows is directly proportional to the reaction time. The distance can be varied over the range 0−100 mm with 0.5 mm precision, allowing kinetic studies between 0 and 3.3 ms (the gas speed is around 30 m s^{-1}). The pressure, typically 2 Torr, is measured by a capacitance manometer (Barocel 0−10 Torr), and the flow rates are adjusted by thermal mass flow controllers (Tylan).

CH radicals were produced from the $CHBr_3 + 3\ K \rightarrow CH + 3\ KBr$ overall reaction which can be separated into three elementary bromine abstractions. As all of the $K + CHBr_x \rightarrow KH + CBr_x$ ($x \geq 0$) reactions are endoergic, this source can only produce CH radicals. As the sum of the exothermicities of the three abstractions[25,26] is 208 kJ mol^{-1}, the production of CH($a^4\Sigma^-$) radicals which is 69.9 kJ mol^{-1} above the ground state, is possible. However, that would require a high concentration of metastable species with long lifetimes (such as electronically excited CHBr) in the oven, which is unlikely in our conditions. Moreover, the CH($a^4\Sigma^-$) reactivity is negligible compared to the CH($X^2\Pi$) reactivity toward alkane.[27] As a large excess of potassium is introduced in the injector compared to the $CHBr_3$ concentration, the precursors ($CHBr_3$, $CHBr_2$, and CHBr) concentrations in the fast flow reactor are very small and will not interfere in our study, as well as K atoms which are not reactive with alkane molecules. The typical conditions in the reactor are the following: $P = 2$ Torr, [K] < 0.1 mTorr, [$CHBr_3$, $CHBr_2$, and CHBr] ≪ 0.001 mTorr, and [CH] ≈ 0.3 mTorr (1.0×10^{11} molecules cm^{-3}). $CHBr_3$ (99%) was used without any further purification. The different alkanes were used directly from the cylinder with a purity of >99%. The carrier gas He had a stated purity of 99.995%.

The CH radicals are probed by LIF using a ND:YAG laser (Quantel YG 581C) pumped dye laser (around 100 μJ by pulse) exciting the CH ($A^2\Delta \leftarrow X^2\Pi$) transition near 431 nm or by OH ($A^2\Sigma \rightarrow X^2\Pi$) chemiluminescence detection with an interferential filter around 305 nm, with electronically excited OH being produced by introducing a very minor amount of O_2 for kinetics experiments (kinetic contribution of the CH + O_2 reaction is always inferior to 5% of the CH + alkane contribution).

Hydrogen atoms are detected by resonance fluorescence using the $2p^1\ ^2P_0 \rightarrow 1s^1\ ^2S$ transition at 121.6 nm. Atom excitation is achieved with the microwave discharge lamp previously described.[1,2,21,22] We also use the microwave discharge lamp in an absorption setup to check the absorption of H atoms and alkanes in the reactor. Typically, the maximum H atom absorption at the L_α is 3%, which corresponds to about 4×10^{10} molecule cm^{-3} with our microwave lamp conditions, and the absorption by alkanes is always inferior to 0.1%. Thus, the conditions of the presently reported experiments ensure the linear dependence of the atomic fluorescence signal versus the lamp emission intensity or the H atoms concentration and also the negligible influence of the alkane absorption.

III. Results

A. Overall Rate Constant. The pseudo-first-order decays of the CH radical fluorescence signal were monitored at different concentrations of alkanes introduced in large excess. To get rid of the mixing effects, only the last stages of the decay (after 3 cm from the injector exit) have been taken to determine the pseudo-first-order rate constants. The measured rate constants were then corrected for radial and axial diffusion from Keyser's formula,[28] as done previously with good results.[1]

A typical measurement of the pseudo-first-order rate constant is displayed in Figure 1, for the CH + C_3H_8 reaction, where axial and radial corrected pseudo-first-order rate constants are plotted versus the alkane concentrations. The main source of errors in our measurements is the important radial and axial diffusions corrections. Moreover, the high wall removal rate constant, due to wall deposit of potassium, associated with these diffusions, leads to the limit conditions of the plug-flow approximation, and the errors quoted take into account these uncertainties. The second-order rate constants of CH reactions with the alkanes concerned obtained in this study are summarized in Table 1 and are compared with previous measurements. The present results are in fairly good agreement with the previous work considering the variety of experimental setups.

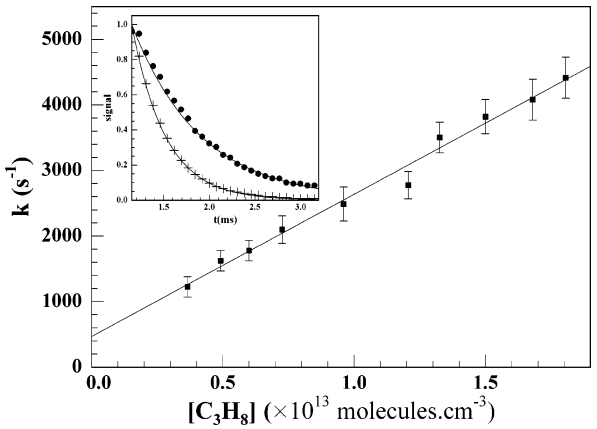

Figure 1. Pseudo-first-order rate constant for the CH + C_3H_8 reaction versus the C_3H_8 concentration. The gradient of the fitted linear dependence yields the second-order rate constant, $k = (2.20 \pm 0.8) \times 10^{-10}$ cm^3 $molecule^{-1}$ s^{-1} at $T = 300$ K and $P = 2.0$ Torr in He. The inset shows two typical CH decay signals, one from CH LIF signal (full dot) with 3.66×10^{12} molecule cm^{-3} of C_3H_8 and one from OH* chemiluminescence signal (cross) with 1.20×10^{13} molecule cm^{-3} of C_3H_8.

TABLE 1: Overall Rate Constants at Room Temperature in 10^{-10} cm^{-3} $molecule^{-1}$ s^{-1}

reactions	k_{298K} in units of 10^{-10} $cm^{-3}molecule^{-1}s^{-1}$	ref
CH + CH_4	0.76 ± 0.20	1
	0.94 ± 0.20	39
	0.66 ± 0.03	40
	0.90 ± 0.20	41
	0.54 ± 0.10	12
	0.97 ± 0.10	13
	1.00 ± 0.30	11
CH + C_2H_6 (ethane)	1.60 ± 0.60	2
	2.39 ± 0.19	11
	2.80 ± 0.30	12
	4.00 ± 0.80	14
CH + C_3H_8 (propane)	2.20 ± 0.80	this study
	4.12 ± 0.13	15
	1.36 ± 0.33	16
CH + C_4H_{10} (n-butane)	2.80 ± 0.80	this study
	4.80 ± 0.80	12
	5.80 ± 0.52	13
CH + C_5H_{12} (n-pentane)	3.20 ± 0.80	this study
	5.03 ± 0.10	15
CH + C_5H_{12} (neo-pentane)	3.30 ± 0.60	this study
CH + C_6H_{14} (n-hexane)	3.60 ± 0.80	this study

B. Product Branching Ratio. Hydrogen atom productions by the CH + alkane reactions were determined relative to H production from the CH + CH_4 reaction by resonance fluorescence in the vacuum ultraviolet. As the H atom branching ratio is known to be 100% in our conditions for the CH + CH_4 reaction,[1] the determination of the branching ratio for CH + alkane reactions thus gives absolute values.

To measure the relative H atom production, the fluorescence signal is recorded successively for CH + CH_4 and CH + alkane reactions. The CH_4 and alkane concentrations were adjusted in order to have equivalent global first-order rate constants, the CH production being constant during a period of more than 1 h. This operation was repeated several times, alternately for different CH_4 and alkane concentrations, under different pressures and different $CHBr_3$ concentrations. In our experimental conditions, we have to take care to check which secondary reactions occur. The main one is the CH + CH → C_2H + H reaction. Other ones could be the C_2H + alkane reactions. However, as these reactions are 10 times slower than the CH + alkane reactions and also only lead to direct H atom abstraction,[29,30] they can be neglected. Finally, there are the alkane reactions with molecules and radicals produced by the CH + alkane reactions. However, the CH + alkanes reactions produce alkene, alkyl radicals, or hydrogen atoms which do not react with alkane in our experimental conditions. These reactions are therefore slow enough to be neglected. So the only main secondary chemical source of H atoms considered here is the CH + CH → C_2H + H reaction, which produces typically 10% of the total amount of H atoms from the initial CH concentration. To determine the H atom production of the CH + alkane reactions, we performed simulations of H production, including the CH + CH → C_2H + H reaction, mixing effects, and wall reactions, for each system: CH alone, CH + CH_4, and CH + alkane. The contribution from the CH + CH reaction, when CH_4 or alkane is added has been described and validated in our previous article.[2] This contribution is calculated by integrating the C_2H* chemiluminescence signal convoluted with the wall loss rate constant of 300 s^{-1} for H atoms in our experimental conditions (this fast loss of H atoms is due to the high reactivity of H atoms with the potassium deposited on the wall). This contribution is then scaled with the H production signal when only CH radicals are present in the reactor using the C_2H* chemiluminescence integration ratio. The fitted parameter was the product branching ratio of H atom production of the CH + alkane reaction. Typical traces of H atom concentrations, deduced from the fluorescence signals, versus the distance (i.e., the reaction time) are shown in Figure 2 for the CH + *n*-C_5H_{12} reaction. Our experimentally determined H atom branching ratios are presented in Table 2.

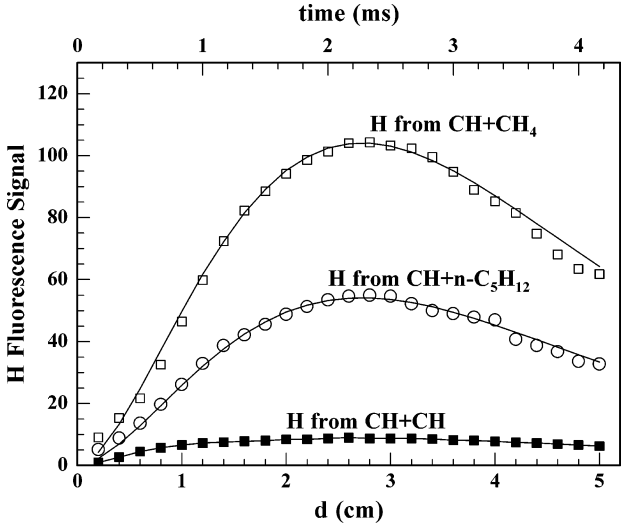

Figure 2. H fluorescence signals from the reaction of the CH radical with CH_4 or *n*-C_5H_{12}. The concentrations were adjusted to have the same pseudo-order rate constant: (a) open squares, H production from the CH + CH_4 reaction, (b) open circles, H production from the CH + C_5H_{12} reaction, and (c) filled squares, H production contribution from the CH + CH reaction during the CH + CH_4 or CH + *n*-C_5H_{12} reactions. The fits linking the H production plot result from a global simulation of the different reactions (see text).

TABLE 2: Branching Ratio of Atomic Hydrogen

reactions	H atom yield	ref
CH + CH_4	1.00	1
CH + C_2H_6 (ethane)	0.22 ± 0.08	2
	0.14 ± 0.06	19
CH + C_3H_8 (propane)	0.19 ± 0.07	this study
CH + C_4H_{10} (n-butane)	0.14 ± 0.06	this study
CH + C_5H_{12} (n-pentane)	0.52 ± 0.08	this study
CH + C_5H_{12} (neo-pentane)	0.51 ± 0.08	this study
	−0.10 ± 0.12	19
CH + C_5H_{12} (iso-pentane)	0.12 ± 0.06	this study
CH + C_6H_{14} (n-hexane)	0.06 ± 0.04	this study

IV. Discussion

A. Overall Rate Constant. The use of the same apparatus under the same pseudo-first-order conditions for the measurements of the global rate constants lead to small relative uncertainties. So comparisons can be easily made, as well as quantification of the regular increase of the rate constants with the size of the alkanes. The high values of the rate constants for these reactions suggest that there are no barriers on the potential energy surfaces for those reactions. This absence of a barrier is confirmed for the CH + CH_4 and CH + C_2H_6 reactions by the low-temperature kinetics studies performed at Rennes with the CRESU technique.[11,17,18] As shown by ab initio calculations for CH + methane[1] and CH + ethane,[2] the first step is the insertion of the CH radical into an alkane C−H bond, resulting in a chemically activated alkyl radical. This transient radical rapidly decomposes. As the threshold energy of this decomposition step is much lower than the energy of the entrance channel, the lifetime of the alkyl radical adduct is very short (typically 10^{-11} s). Therefore, the rate determining process is the CH insertion. The same argument can be applied to a CH radical reacting with larger alkanes. The experimental increase of the rate constants, which vary with the size of the alkane reactant, is, consequently, due to the increase of the collision cross section. As there is no activation barrier during the CH radical insertion, we can apply classical capture theory. As alkanes are nonpolar molecules, the main term in the long range interaction potential is the isotropic dispersion one: $-C_6/R^6$.[31] Using the same methodology as Clary[32] for C + alkene and C + alkyne reactions, the overall rate constant at a given temperature is proportional to the cubic root of the C_6 coefficient and, consequently, proportional to the cubic root of the alkane isotropic polarizability.[32] As such, polarizabilities are proportional to the number *N* of carbon atoms in the molecules,[33] and the rate constant at room temperature (298 K) is directly proportional to $N^{1/3}$. Figure 3 plots the experimental rate constants versus $N^{1/3}$. The linear dependence provides clear evidence that capture theory appropriately describes these reactions which are, indeed, mostly controlled by long-range intermolecular forces. However, we point out the limits of the procedure used to fit the rate constants which uses only isotropic dispersion terms in the interaction potential.

B. Product Branching Ratio. The H branching ratios are low and inversely proportional to the alkane's size, with the notable exceptions of the CH + *n*-pentane and CH + neopentane reactions (see Table 2). Despite the variety of mechanisms available in such complex systems, we could use the previous theoretical study of the reaction prototype CH + C_2H_6[2]

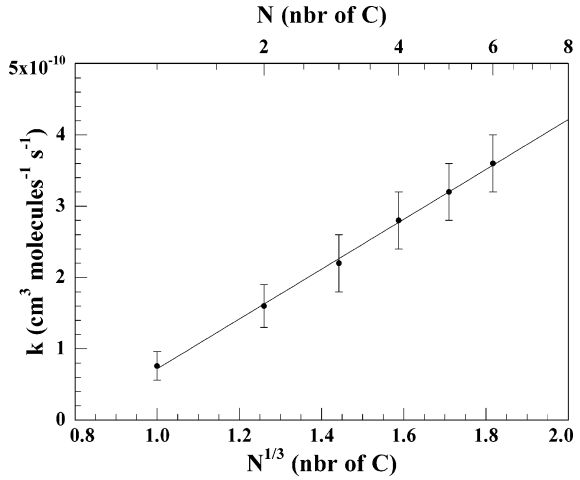

Figure 3. Plot of the experimental rate constant for the reactions of ground state CH radicals with *n*-alkanes versus $N^{1/3}$, *N* being the number of carbon atoms of the *n*-alkanes.

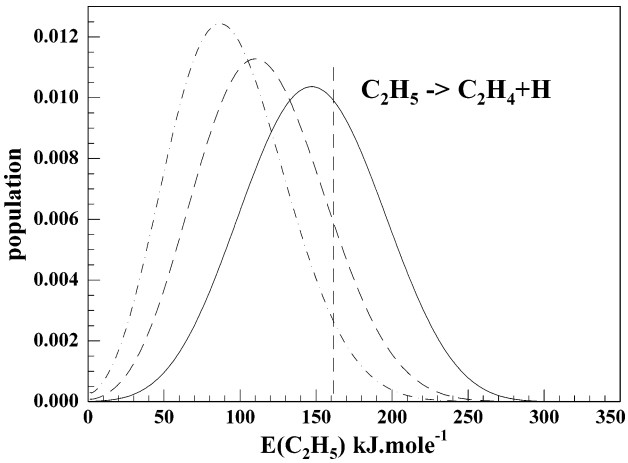

Figure 4. Calculated nascent population distribution of C_2H_5 produced by CH + C_3H_8 → 1-C_4H_9 → C_2H_5 + C_2H_4. (continuous curve), produced by CH + C_4H_{10} → 1-C_5H_{11} → C_2H_5 + 1-C_3H_6. (dash curve), and produced by CH + C_5H_{12} → 1-C_6H_{13} → C_2H_5 + 1-C_4H_8. (dash-dot curve). The dashed line indicates the threshold dissociation energy.

and thermal decomposition of the alkyl radical[23,34] to explain the general trend. The key steps are as follows:

(1) Insertion into the alkane CH bond is the major attack step (insertion in a CC bond being unfavorable because of the steric hindrance).[2]

(2) The produced alkyl adduct has a large excess of energy, a narrow energy distribution, and an estimated lifetime close to 10^{-11} s,[2] which has to be compared with a collision frequency close to 3×10^7 s^{-1} at 2 Torr, so, the collisional stabilization of this adduct at 2 Torr is negligible.[2]

(3) The 1,2 or 1,3 isomerization reactions are minor in C_3 and C_4 alkyl radicals but 1,4, 1,5, or 1,6 isomerization reactions appear in C_5, C_6, and C_7 alkyl radicals with rate constants similar to the direct C−C fission.[23,34]

(4) βC−C bond cleavage always dominates over βC−H bond cleavage. The C−C bond fission is always favored because the threshold energy for the C−C fission and the C−H fission channels are typically around 125 and 150 kJ mol^{-1} respectively.[23]

(5) βC−C bond fission leads to the production of an alkene and an alkyl radical, the latter one can itself dissociate in some cases.

CH + C_3H_8. The experimental H production for this reaction is equal to 19%. This low H atom branching ratio is consistent with the fact that direct H atom channels play a minor role. The insertion of the CH radical into one CH bond of *n*-propane can form either an *n*-butyl radical ($CH_3CH_2CH_2CH_2^•$) or an *i*-butyl radical ($(CH_3)_2CHCH_2^•$). The evolution of these two alkyl radicals can lead to (thermodynamic data are derived from refs 33, 35, and 36)

$$\mathrm{CH} + \mathrm{C_3H_8} \rightarrow n\text{-}\mathrm{C_4H_9} \rightarrow \mathrm{C_2H_4} + \mathrm{C_2H_5} \qquad \Delta_r H^0_{298} = -319 \text{ kJ mol}^{-1} \quad (1a)$$

$$1\text{-}\mathrm{C_4H_8} + \mathrm{H} \qquad \Delta_r H^0_{298} = -285 \text{ kJ mol}^{-1} \quad (1b)$$

$$\mathrm{CH} + \mathrm{C_3H_8} \rightarrow i\text{-}\mathrm{C_4H_9} \rightarrow \mathrm{C_3H_6} + \mathrm{CH_3} \qquad \Delta_r H^0_{298} = -325 \text{ kJ mol}^{-1} \quad (1c)$$

$$i\text{-}\mathrm{C_4H_8} + \mathrm{H} \qquad \Delta_r H^0_{298} = -291 \text{ kJ mol}^{-1} \quad (1d)$$

As for our previous study of the CH + C_2H_6 reaction,[2] ab initio studies of the different stationary points relevant to this reaction and RRKM calculations, including tunneling effects, of the various steps of the mechanism were performed. This study is detailed elsewhere[37] and only the results are presented here. As the threshold energy for three- and four-member ring isomerization is higher than for C−H fission with a tighter transition state, there is no possibility of isomerization for *n*-butyl and *i*-butyl radicals. To obtain the branching ratio of the various products, the differential equation system describing the kinetic evolution of the butyl radicals has been solved using the calculated microcanonical constants. For the *n*-C_4H_9 decomposition, calculations give 95% for the C_2H_4 + C_2H_5 channel and 5% for the 1-C_4H_8 + H channel, and for the *i*-butyl radical decomposition, calculations give 96% for the C_3H_6 + CH_3 channel and 4% for the *i*-C_4H_8 + H channel. In both cases, the H channels are unfavorable because of the higher activation energy (20−30 kJ mol^{-1}) of the butyl decomposition routes. This calculated H atom production is also much lower than the experimental one (19%). The higher experimental H atom production is likely to be explained by prompt dissociation of alkyl radical products. As the CH_3 radical is produced with an internal energy inferior to its C−H bond energy (462 kJ mol^{-1}),[33] the only secondary source of H atoms is the C_2H_5 radical produced by reaction 1a. The exothermicity of the CH + C_3H_8 → *n*-C_4H_9 → C_2H_4 + C_2H_5 reaction is $\Delta_r H^0_{298} = -319$ kJ mol^{-1} and the energy threshold dissociation of the C_2H_5 radical (leading to C_2H_4 + H) is localized 155 kJ mol^{-1} higher than the C_2H_5 energy. The amount of dissociated C_2H_5 has been estimated by calculating the amount of C_2H_5 prompt dissociation from the nascent population of C_2H_5 above the dissociation limit based on the prior distribution, including collisional stabilization, of the *n*-C_4H_9 → C_2H_4 + C_2H_5 reaction. An RRKM-Master equation procedure was used[38] where the average energy lost in deactivating collisions $\langle\Delta E\rangle_{down}$, was kept equal to 180 cm^{-1}, a reasonable value for He buffer gas. The C_2H_5 nascent population distribution, produced by reaction 1a is presented in Figure 4. The pressure dependence of the C_2H_5 prompt dissociation process is presented in Table 3. The C_2H_5 prompt dissociation from the nascent population of C_2H_5 above dissociation is equal to 40 ± 3% (the error is calculated taking into account the errors in $\Delta_f H^0_{298}$ of the various species) and the amount of dissociated C_2H_5 is equal to 35 ± 5% at 2 Torr of He (our experimental conditions; the error is calculated taking into account the errors in $\Delta_f H^0_{298}$ and the error in $\langle\Delta E\rangle_{down}$

TABLE 3: Amount of Prompt C_2H_5 Dissociation, from CH + C_3H_8 → 1-C_4H_9 → C_2H_5 + C_2H_4, and *t*-C_4H_9 Dissociation, from CH + neo-C_5H_{12} → C_6H_{13} → *t*-C_4H_9 + C_2H_4, at Various Pressures of He

P(Torr)	% of dissociated C_2H_5	% of dissociated t−C_4H_9
0.001	40	94
0.01	39	88
0.1	38	81
2	35	60
25	25	26

taken equal to ±80 cm^{-1}). After fitting our experimental value of 19 ± 7% for the total H atom production, we obtained 44 ± 17% of *n*-C_4H_9 formation and 56 ± 17% of *i*-C_4H_9 formation for the CH + C_3H_8 reaction. These results are quite surprising considering the statistical weight of the CH radical insertion into an alkane C−H bond leading to 75% of *n*-C_4H_9 (6/8) and 25% of *i*-C_4H_9 (2/8). This result could be due to the fact that, for the CH radical attack, the central part of the propane molecule is more attractive than the outer part, decreasing the probability of CH insertion into the terminal CH bonds (i.e., *n*-C_4H_9 production). The final product ratios of the CH + C_3H_8 reaction, including secondary prompt dissociation given by the fit of the experimental H production, are C_3H_6 (52%), CH_3 (52%), C_2H_4 (44%), C_2H_5 (30%), and H (19%).

CH + C_4H_{10}. The experimental H production for this reaction is equal to 14%. This result is also in agreement with the fact that direct H atom channels play a minor role. The insertion of the CH radical into one CH bond of the *n*-butane could lead either to a 1-pentyl radical ($CH_3CH_2CH_2CH_2CH_2^•$) or a 2-methylbutyl radical ($CH_3CH_2CH(CH_3)CH_2^•$) (i-C_5H_{11}). The evolution of these two alkyl radicals can lead to (thermodynamic data are taken from refs 33, 35, and 36 with the zero energy corresponding to the energy of the reactants CH + C_4H_{10} in their ground states)

$$1\text{-}^•C_5H_{11} \rightarrow C_2H_4 + n\text{-}C_3H_7 \qquad \Delta_rH^0_{298} = -317 \text{ kJ mol}^{-1} \tag{2a}$$

$$n\text{-}C_5H_{10} + H \qquad \Delta_rH^0_{298} = -273 \text{ kJ mol}^{-1} \tag{2b}$$

$$i\text{-}^•C_5H_{11} \rightarrow C_4H_8 + CH_3 \quad \Delta_rH^0_{298} = -334 \text{ kJ mol}^{-1} \tag{2c}$$

$$C_3H_6 + C_2H_5 \qquad \Delta_rH^0_{298} = -330 \text{ kJ mol}^{-1} \tag{2d}$$

$$i\text{-}C_5H_{10} + H \qquad \Delta_rH^0_{298} = -288 \text{ kJ mol}^{-1} \tag{2e}$$

In every case, the H channels are unfavorable because of a higher exit transition state energy (40 kJ mol^{-1}) and the direct H atom production is certainly lower than or equal to 5% by comparison with the CH + C_3H_8 study. As five-membered ring 1,4 primary to secondary isomerization is competitive with C−H and C−C bond dissociations, a part of the 1-$^•C_5H_{11}$ will isomerize into 2-$^•C_5H_{11}$. For the 2-$^•C_5H_{11}$ evolution, C−H bond dissociation is very inefficient, and the decomposition of 2-$^•C_5H_{11}$ leads mainly to C_3H_6 + C_2H_5. The direct H atom production is then very low (around 5%), and the main source of H atoms comes from prompt dissociation. For *n*-C_3H_7 dissociation, we have calculated, using the micocanonical rate constants obtained previously[2] and assuming a statistical energy distribution for *n*-C_3H_7 formation, that 92% of the *n*-C_3H_7 is dissociated leading to 88% of CH_3 + C_2H_4 and 4% of H + C_3H_6. Another source of H atoms is the dissociation of the C_2H_5 radical. C_2H_5 is produced either by the dissociation of *i*-$^•C_5H_{11}$, or by the decomposition of 2-$^•C_5H_{11}$ formed from the isomerization of 1-$^•C_5H_{11}$. The energy available in C_2H_5 in this case is similar to the case of CH + C_3H_8. However, as the coproduct is larger for the CH + C_4H_{10} reaction (C_3H_6) than for the CH + C_3H_8 reaction (C_2H_4), the statistical distribution energy in C_2H_5 is shifted toward low energy, and then the amount of prompt C_2H_5 dissociation is smaller. The amount of dissociated C_2H_5 was calculated equal to 12%, the C_2H_5 nascent population distribution, produced by reaction 2d is presented in Figure 4. If 6% of H atoms are produced directly and from the dissociation of *n*-C_3H_7, 8 ± 3% come from C_2H_5 dissociation, which implies that the total C_2H_5 production is around 60 ± 26%. Even if RRKM coupled ab initio calculations are necessary to fully describe this system, the global behavior is well understood. The effective products of the CH + C_4H_{10} reactions are C_2H_4, CH_3, C_4H_8, C_3H_6, and C_2H_5.

CH + *n*-C_5H_{12}. The experimental H production for this reaction is equal to 52%. This result is not in agreement with the fact that direct H atom channels play a minor role due to the much favored C−C bond rupture rather than a C−H bond rupture of the alkyl radical. This unusual result could be due to a high production of a specific alkyl radical followed by a prompt dissociation leading to a H atom (such as from the *t*-C_4H_9 radical) or due to the existence of a new H atom channel. The insertion of the CH radical into one CH bond of *n*-pentane leads either to a 1-hexyl radical ($CH_3CH_2CH_2CH_2CH_2CH_2^•$) (1-$C_6H_{13}$), a 2-methyl-pentyl radical ($CH_3CH_2CH_2CH(CH_3)CH_2^•$) (2-$CH_3C_5H_{10}$), or a 2-ethyl-propyl radical ($CH_3CH_2CH(C_2H_5)CH_2^•$) (i-C_6H_{13}). As five and six membered ring 1,4 and 1,5 primary to secondary isomerizations are competitive with C−H and C−C bond dissociation, some of these alkyl radicals will isomerize leading to a complex alkyl radical distribution. As in the case of CH + C_3H_8 and CH + C_4H_{10} studies, the direct H atom productions are unfavorable because of the higher exit transition state energy (20−40 kJ mol^{-1}),[23,24] and it was estimated to be around 5%. Taking into account the 1,4 and 1,5 isomerizations, the exit channels of the CH + C_5H_{12} reaction are then

$$CH_3CH_2CH_2CH_2CH_2CH_2^• \rightarrow n\text{-}C_4H_9^• + C_2H_4 \tag{3a}$$

$$\rightarrow CH_3CH^•CH_2CH_2CH_2CH_3 \rightarrow C_3H_6 + n\text{-}C_3H_7^• \tag{3b}$$

$$\rightarrow CH_3CH_2CH^•CH_2CH_2CH_3 \rightarrow C_4H_8 + C_2H_5^• \tag{3c}$$

$$\rightarrow {}^•CH_3 + C_5H_{10} \tag{3d}$$

$$CH_3CH_2CH_2CH(CH_3)CH_2^• \rightarrow C_3H_6 + n\text{-}C_3H_7^• \tag{3e}$$

$$\rightarrow {}^•CH_3 + 1\text{-}C_5H_{10} \tag{3f}$$

$$\rightarrow {}^•CH_2CH_2CH_2CH(CH_3)CH_3 \rightarrow C_2H_4 + i\text{-}C_4H_9^• \tag{3g}$$

$$\rightarrow CH_3CH^•CH_2CH(CH_3)CH_3 \rightarrow C_3H_6 + i\text{-}C_3H_7^• \tag{3h}$$

$$CH_3CH_2CH(C_2H_5)CH_2^• \rightarrow C_4H_8 + C_2H_5^• \tag{3i}$$

$$\rightarrow {}^•CH_2CH_2CH_2CH(CH_3)CH_3 \rightarrow C_2H_4 + 2\text{-}C_4H_9^• \tag{3j}$$

Among all of the various alkyl radicals eventually produced, the only sources of H atoms from their prompt dissociation are C_2H_5 (giving C_2H_4 + H), *n*-C_4H_9 (giving C_2H_4 + C_2H_5 followed by C_2H_5 → C_2H_4 + H), and *i*-C_3H_7 (giving C_3H_6 + H). The amount of dissociated C_2H_5 is calculated equal to 4%, and the C_2H_5 nascent population distribution, produced by reaction 3c, is presented in Figure 4. So, most of the H atoms come from the dissociation of *i*-C_3H_7, estimated to be equal to 45%. These results explain a slightly higher H atom production than for the

CH + butane reaction considering that several opened channels could lead to H atom production by alkyl radical dissociations. Taking into account only C−C bond rupture and 1,4 and 1,5 isomerizations, we obtain 12 different exit channels, 4 exit channels producing C_2H_5 radicals, and 1 exit channel producing *i*-C_3H_7 radicals. However the C_2H_5 and *i*-C_3H_7 prompt dissociations cannot explain the very high experimentally observed H atom production (52 ± 8%). Indeed, the percentage of dissociated C_2H_5 and *i*-C_3H_7 is less than 50%, and there are other open exit channels without H production, such as CH_3 production. For example, from the study of Yamauchi,[23] 1,5 isomerization of 1-C_6H_{13}, leading to C_3H_6 + *n*-$C_3H_7^{\bullet}$, occurs at a similar rate to decomposition at high temperatures.

The other possibility for the high H atom branching ratio is the existence of a "new" channel producing H atoms. This channel could be the most exothermic exit channel for the 1-C_6H_{13} evolution: the formation of cyclohexane (*c*-C_6H_{12}) + H localized −354 kJ.mol^{-1} below the reactants and −16 kJ.mol^{-1} below the second most exothermic channel (C_4H_8 + $C_2H_5^{\bullet}$). Unfortunately, ab initio calculations show that the exit transition state of this channel is located much higher than for other exit channels and has a much tighter structure. So, this channel should play a minor role even considering the tunneling effect. New ab initio calculations are currently being performed on all of the intermediates and products of this system to obtain a better understanding of it.

CH + neo-C_5H_{12}. The experimental H production for this reaction is equal to 51%, similar to the CH + *n*-C_5H_{12} one. This result is not in agreement with the fact that direct H atom channels play a minor role due to the much favored C−C bond rupture rather than C−H bond rupture of an alkyl radical, and moreover, it is also not in agreement with the experimental determination by McKee and al[19] which is equal to −0.10 ± 0.12, then close to zero.

As all of the CH bonds of neo-pentane are equivalent and neglecting C−C bond insertion, the reaction of the CH radical with neo-pentane yields $(CH_3)_3CCH_2CH_2^{\bullet}$ by insertion of the CH radical into one CH bond of the neo-pentane. As C−H bond breaking and 1,2 and 1,3 H atom transfers are not competitive with C−C bond dissociation, $(CH_3)_3CCH_2CH_2^{\bullet}$ would decompose to C_2H_4 + *t*-C_4H_9 (C−C bond rupture) or isomerize to $^{\bullet}CH_2C(CH_3)_2CH_2CH_3$ after 1,4 H atom transfer. The main possible reactive pathways are then

$$(CH_3)_3CH_2CH_2^{\bullet} \rightarrow t\text{-}C_4H_9^{\bullet} + C_2H_4 \quad (4a)$$

$$\rightarrow {}^{\bullet}CH_2C(CH_3)_2CH_2CH_3 \rightarrow C_4H_8 + C_2H_5^{\bullet} \quad (4b)$$

$$\rightarrow C_5H_{10} + {}^{\bullet}CH_3 \quad (4c)$$

In this case, C_2H_5 could produce not only secondary H atoms by prompt dissociation but also *t*-C_4H_9 radicals. The nascent population distribution of the *t*-C_4H_9 produced by (4a) is presented in Figure 5, and the amount of *t*-C_4H_9 prompt dissociation at various pressures is presented in Table 3. At our experimental pressure, 2 Torr, 60% of the *t*-C_4H_9 are dissociated and 4% of the C_2H_5 are dissociated, so the high experimental H atom production could be explained with adequate branching ratios, namely 85% giving of *t*-$C_4H_9^{\bullet}$ + C_2H_4 production. McKee et al. obtained a much lower H atom production,[19] namely near 0%, but they were working at higher pressure (25 Torr of He) for which the stabilization of the *t*-C_4H_9 radical (and also C_2H_5) is higher and so the dissociation toward C_4H_8 + H correspondingly much lower. RRKM calculations give, at 25 Torr, 26% of the dissociated *t*-C_4H_9 and 2% of the dissociated C_2H_5. Thus, the H atom production in the McKee experiment is expected to be close to 22%, higher than their result. However, collisional stabilization of *t*-C_4H_9 could be more efficient in their experiment as they used a higher neo-C_5H_{12} concentration, which is a more efficient collider than He.

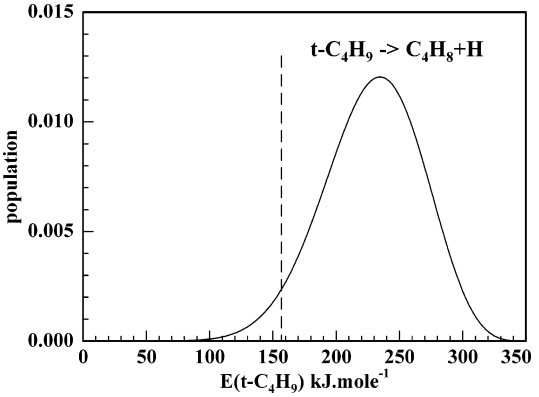

Figure 5. Calculated nascent population distribution of *t*-C_4H_9, produced by CH + C_5H_{12} → C_6H_{13} → *t*-C_4H_9 + C_2H_4. The dashed line indicates the threshold dissociation energy.

CH + iso-C_5H_{12} (2-Methyl-Butane). For this other pentane isomer, the experimental H production is equal to 12%. This result is more in agreement with the fact that direct H atom channels play a minor role due to the much favored C−C bond rupture rather than C−H bond rupture of an alkyl radical. The insertion of the CH radical into one CH bond of the iso-pentane could lead to four isomers. Taking into account only C−C bond rupture and 1,4 and 1,5 isomerizations, we obtain 13 different exit channels. Among them, only two exit channels produce an alkyl radical, C_2H_5, able to produce a H atom by prompt dissociation. The low experimental H atom production seems to be consistent, 5% coming directly from the intermediate alkyl radicals and around 7% coming from the C_2H_5 dissociation.

CH + *n*-C_6H_{14}. For this reaction, the experimental H production is equal to only 6%. This result is in agreement with the fact that direct H atom channels play a minor role due to the much favored C−C bond rupture rather than C−H bond rupture of an alkyl radical. The insertion of the CH radical into one CH bond of the *n*-hexane could lead to various isomers, and considering the 1,4, 1,5, and 1,6 isomerizations pathways, we obtain a quite complex system. The low experimental H atom production seems to indicate that small amounts of C_2H_5, *i*-C_3H_7, or *t*-C_4H_9 are produced and as such there are no major secondary sources of H atom from alkyl prompt dissociations. In this case, calculations will also be required to identify the products of this reaction.

V. Conclusion

In the present study, the first-order rate constants and the H atom branching ratios for the reaction of CH radicals with a series of alkanes from methane to *n*-hexane have been investigated experimentally. The high values and the increase of the rate constants with the size of the alkane are predicted from a simple classical capture theory with a single dispersion term for the potential energy surface. The experimental decrease of H atom production with the size of alkane is related to the decrease of the direct H atom channel occurrence, due to the much favored C−C bond rupture rather than C−H bond rupture of an alkyl radical. However, the H atom production is in general higher than the calculated direct one because of prompt dissociation of products, namely C_2H_5, *i*-C_3H_7, and *t*-C_4H_9. RRKM predictions have been performed on CH + C_3H_8 and

will be developed in a later paper. For one particular reaction, CH + n-C_5H_{12}, the H atom branching ratio could not be explained and should be investigated by further theoretical studies.

References and Notes

(1) Fleurat-Lessard, P.; Rayez, J. C.; Bergeat, A.; Loison, J. C. *Chem. Phys.* **2002**, *279*, 87.
(2) Galland, N.; Caralp, F.; Hannachi, Y.; Bergeat, A.; Loison, J.-C. *J. Phys. Chem. A* **2003**, *107*, 5419.
(3) Sanders, W. A.; Lin, M. C. In *Chemical Kinetics of Small Organic Radicals*; Alfassi, Z. B., Ed.; CRC: Boca Raton, FL, 1986; Vol. III.
(4) Herbst, E.; Lee, H.-H.; Howe, D. A.; Millar, T. J. *Mon. Not. R. Astron. Soc.* **1994**, *268*, 335.
(5) Lebonnois, S.; Toublanc, D.; Hourdin, F.; Rannou, P. *Icarus* **2001**, *152*, 384.
(6) Yelle, R. V.; Herbert, F.; Sandel, B. R. *Icarus* **1993**, *104*, 38.
(7) Krasnopolsky, V. A.; Cruikshank, D. P. *J. Geophys. Res. E* **1995**, *100*, 21271.
(8) Mordaunt, D. H.; Lambert, I. R.; Morley, G. P.; Ashfold, M. N. R.; Dixon, R. N.; Schnieder, L.; Welge, K. H. *J. Chem. Phys.* **1993**, *98*, 2054.
(9) Wang, J. H.; Liu, K.; Min, Z.; Su, H.; Bersohn, R.; Preses, J.; Larese, J. Z. *J. Chem. Phys.* **2000**, *113*, 4146.
(10) Wayne, R. P. *Chemistry of Atmospheres*; Clarendon Press: Oxford, 1991.
(11) Canosa, A.; Sims, I. R.; Travers, D.; Smith, I. W. M.; Rowe, B. R. *Astron. Astrophys.* **1997**, *323*, 644.
(12) Berman, M. R.; Lin, M. C. *Chem. Phys.* **1983**, *82*, 435.
(13) Butler, J. E.; Fleming, J. W.; Goss, L. P.; Lin, M. C. *Chem. Phys.* **1981**, *56*, 355.
(14) Butler, J. E.; Fleming, J. W.; Goss, L. P.; Lin, M. C. *Am. Chem. Soc. Symp. Ser.* **1980**, *134*, 397.
(15) Zabarnick, S.; Fleming, J. W.; Lin, M. C. *Chem. Phys.* **1987**, *112*, 409.
(16) Bosnali, M. W.; Perner, D. *Z. Naturforsh.* **1971**, *26 a*, 1768.
(17) Chastaing, D.; James, P. L.; Sims, I. R.; Smith, I. W. M. *Phys. Chem. Chem. Phys.* **1999**, *1*, 2247.
(18) Chastaing, D.; Le Picard, S. D.; Sims, I. R.; Smith, I. W. M.; Geppert, W. D.; Naulin, C.; Costes, M. *Chem. Phys. Lett.* **2000**, *331*, 170.
(19) McKee, K.; Blitz, M. A.; Hughes, K. J.; Pilling, M. J.; Qian, H.-B.; Taylor, A.; Seakins, P. W. *J. Phys. Chem.* **2003**, *107*, 5710.
(20) Taatjes, C. A.; Klippenstein, S. J. *J. Phys. Chem. A* **2001**, *105*, 8567.
(21) Bergeat, A.; Calvo, T.; Daugey, N.; Loison, J.-C.; Dorthe, G. *J. Phys. Chem. A* **1998**, *102*, 8124.
(22) Bergeat, A.; Calvo, T.; Caralp, F.; Fillion, J. H.; Dorthe, G.; Loison, J. C. *Faraday Discuss.* **2002**, *119*, 67.
(23) Yamauchi, N.; Miyoshi, A.; Kosada, K.; Koshi, M.; Matsui, H. *J. Phys. Chem. A* **1999**, *103*, 2723.
(24) Viskolcz, B.; Lendvay, G.; Körtvelyesi, T.; Seres, L. *J. Am. Chem. Soc.* **1996**, *118*, 3006.
(25) Born, M.; Ingemann, S.; Nibbering, N. M. M. *J. Am. Chem. Soc.* **1994**, *116*, 7210.
(26) Tschuikow-Roux, E.; Paddison, S. *Int. J. Chem. Kinet.* **1987**, *19*, 15.
(27) Hou, Z.; Bayes, K. D. *J. Phys. Chem.* **1993**, *97*, 1896.
(28) Keyser, L. F. *J. Phys. Chem.* **1984**, *88*, 4750.
(29) Ceursters, B.; Nguyen, H. M. T.; Peeters, J.; Nguyen, M. T. *Chem. Phys. Lett.* **2000**, *329*, 412.
(30) Ceursters, B.; Nguyen, H. M. T.; Nguyen, M. T.; Peeters, J.; Vereecken, L. *Phys. Chem. Chem. Phys.* **2001**, *3*, 3070.
(31) Stoecklin, T.; Clary, D. C. *J. Phys. Chem.* **1992**, *96*, 7346.
(32) Clary, D. C. H. N.; Husain, D.; Kabir, M. *ApJ.* **1994**, *422*, 416.
(33) *Handbook of Chemistry and Physics*; CRC Press: Boca Raton, FL, 2001.
(34) Dean, A. M. *J. Phys. Chem.* **1985**, *89*, 4600.
(35) *Third Millennium Ideal Gas and Condensed Phase Thermochemical Database for Combustion. Report TEA867(http://garfield.chem.elte.hu/Burcat/burcat.html)*; Burcat, A., Ed.; 2001.
(36) Turanyi, T.; Zalotai, L.; Dobé, S.; Berces, T. *Phys. Chem. Chem. Phys.* **2002**, *4*, 2568.
(37) Hannachi, Y.; Loison, J. C.; Bergeat, A.; Caralp, F. in preparation **2006**.
(38) Caralp, F.; Forst, W.; Rayez, M. T. *Phys. Chem. Chem. Phys.* **2003**, *5*, 476.
(39) Thiesemann, H.; MacNamara, J.; Taatjes, C. A. *J. Phys. Chem. A* **1997**, *101*, 1881.
(40) Blitz, M. A.; Johnson, D. G.; Pesa, M.; Pilling, M. J.; Robertson, S. H.; Seakins, P. W. *J. Chem. Soc. Faraday Trans.* **1997**, *93*, 1473.
(41) Anderson, S. M.; Freedman, A.; Kolb, C. E. *J. Phys. Chem.* **1987**, *91*, 6272